Scientific Research Publishing

Journal of Modern Physics, 2022, 13, 839-850
https://www.scirp.org/journal/jmp
ISSN Online: 2153-120X
ISSN Print: 2153-1196

Exposure to Long Magnetic Resonance Imaging Thermometry Does Not Cause Significant DNA Double-Strand Breaks on CF-1 Mice

Christopher Brian Abraham[1*], Sepideh Dadgar[2], Wely B. Floriano[2], Michael Campbell[2,3], Laura Curiel[4]

[1]Department of Electrical Engineering, Lakehead University, Thunder Bay, Canada
[2]Department of Chemistry, Lakehead University, Thunder Bay, Canada
[3]Thunder Bay Regional Health Research Institute, Thunder Bay, Canada
[4]Electrical and Computer Engineering, University of Calgary, Calgary, Canada
Email: *cabraham@lakeheadu.ca

How to cite this paper: Abraham, C.B., Dadgar, S., Floriano, W.B., Campbell, M. and Curiel, L. (2022) Exposure to Long Magnetic Resonance Imaging Thermometry Does Not Cause Significant DNA Double-Strand Breaks on CF-1 Mice. *Journal of Modern Physics*, **13**, 839-850.
https://doi.org/10.4236/jmp.2022.136047

Received: March 8, 2022
Accepted: June 7, 2022
Published: June 10, 2022

Abstract

The purpose of the study was to investigate if the high gradient strength and slew rate used for long MRI-thermometry monitoring could cause DNA double-stranded breaks (DSBs). To this end, an enzyme-linked immunosorbent assay (ELISA) was used to quantify γH2AX, a molecular marker for DSBs, in the blood of mice after a 6-hour exposure to magnetic resonance imaging (MRI). Fourteen CF-1 female mice were separated into 4 experimental groups: Untreated negative control, MRI-treated, MRI-Control, and exposed to ionizing radiation positive control. Untreated negative control was used as a baseline for ELISA to quantify γH2AX. MRI-treated consisted of a 6-hour continuous magnetic resonance imaging (MRI) echo planar imaging (EPI) sequence with a slew rate of 192 mT/m/s constituting a significantly longer imaging time than routine clinical imaging. MRI-control mice were maintained under the same conditions outside the MRI scanner for 6-hours. Mice in the irradiation group served as a positive control of DSBs and were exposed to either 2 Gy, 5 Gy or 10 Gy of ionizing radiation. DSBs in the blood lymphocytes from the treatment groups were analyzed using the γH2AX ELISA and compared. Total protein concentration in lysates was determined for each blood sample and averaged 1 ± 0.35 mg/mL. Irradiated positive controls were used to test radiation dose-dependency of the γH2AX ELISA assay where a linear dependency on radiation exposure was observed ($r^2 = 0.93$) between untreated and irradiated samples. Mean and standard error mean of γH2AX formation were calculated and compared between each treatment group. Repeated measures 1-way ANOVA showed statistically significant differences between the means of irradiated controls and both the MRI-control

and MRI-treated groups. There was no statistically significant difference between the MRI-treated samples and the MRI-control groups. Our results show that long MRI exposure at a high slew rate did not cause increased levels of γH2AX when compared to control mice, suggesting that no increase in DSBs was caused by the long MR thermometry imaging session. The novelty of this work contradicts other studies that have suggested MRI may cause DSBs; this work suggests an alternative cause of DNA damage.

Keywords

γH2AX, DNA Damage, MRI Thermometry, Gadolinium, Double-Stranded Breaks (DSBs), ELISA, Ionizing Radiation

1. Introduction

There have been suggestions in the literature that high gradient strengths and high slew rates that are near the maximum allowed by clinical MRI systems could cause double-stranded breaks (DSBs) in DNA, one of the most dangerous types of DNA damage occurring within the cell [1]. A recent review has documented and examined the current literature in detail and has found much of the available data on MRI-induced DSBs conflicting [2]. One publication reported an increase in DNA DSBs when using cardiac magnetic resonance (CMR) [3] and suggested that this type of damage was similar to that caused by X-ray and nuclear imaging techniques. However, this study also used gadolinium injections as a contrast agent, which is currently under heavy scrutiny due to potential effects leading to organ damage [4] [5]. Another publication reported an increase in micronucleus formation that returned to normal values 24 h post-treatment [6]. Using a Comet assay on human lymphocytes obtained from participants undergoing MRI, one group reported an increase in DNA damage when gadolinium was used for contrast enhancement [7]. An increase of chromosome aberrations, micronuclei, and DNA damage were also found with a Comet assay when exposing cultured human lymphocytes to MRI *in vitro* [8]. More recent studies, using γH2AX as a biomarker for DNA damage, have suggested that MRI causes no DNA damage, even at different magnetic field strengths [9] [10] [11]. One study [12] monitored DNA damage using γH2AX over a one-year period following CMR (without the use of gadolinium), and reported DNA damage in T lymphocytes from 2 days until 1-month post-CMR. However, no damage was detected after 1 year. Schreiber et al. tested bacteria at 1.5 T and 7.2 T using a reverse mutation assay method and did not report significant DNA damage [13]. In summary, although there do exist reports suggesting MRI may cause various forms of DNA damage, results are conflicting and may be influenced by secondary sources.

Measuring levels of γH2AX has become the gold standard in radiation biodosimetry for the detection of DSBs [14] [15]. Once a DSB is formed, the histone protein H2AX becomes rapidly phosphorylated at Ser-139, denoted γH2AX [16]

[17]. This biomarker for DSBs has also been verified in mice models and showed high reproducibility in quantifying DNA damage [15] [18]. The accumulation of γH2AX around each DSB appears as a single focus in immunofluorescence microscopy, where the number of foci per cell directly correlates to DSBs per cell and, thus, the degree of DNA damage [19].

Although immunofluorescence-based microscopy is the most sensitive assay to measure DSB levels, it is also the most labour-intensive [20]. Tissue samples must be individually prepared for microscopy where images of hundreds of thousands of cells must be processed and then counted to quantify the γH2AX foci. Although other options exist such as flow cytometry, it suffers from low-throughput and limited sensitivity [21]. An enzyme-linked immunosorbent assay (ELISA) has been developed to detect γH2AX [22]. This highly sensitive assay has been used in recent clinical trials [22] [23]. Johnston *et al.* used an ELISA to monitor γH2AX response in irradiated human blood samples *ex vivo* and mouse embryo fibroblasts over a range of 0-5 Gy [24]. Ji *et al.* optimized the previously mentioned ELISA to accurately measure DSBs induced by ionizing radiation or DNA-damaging agents in both cells and tissues [20].

Our work aims to shed light on the conflicting reports regarding DSBs caused by high gradient strength and high slew rate from MRI, particularly for long sequences used for thermometry. In this study, we exposed mice to a 6-hour long MRI session using the maximum gradient strength and slew rate available for a thermometry sequence. The presence of γH2AX was quantified and compared between animals exposed to MRI, positive controls exposed to radiation and negative controls. DNA damage was quantified by γH2AX levels detected using an ELISA protocol adapted from previously reported protocols [20] [24].

2. Materials and Methods

2.1. Ethics Statement

All experiments involving animals were carried out using protocols approved by the Lakehead University Animal Care Committee (LUACC).

Mice

Fourteen CF-1 female mice weighing 13 - 15 g were purchased (Charles River, Wilmington, MA, USA). After arrival, they were housed at standard conditions according to approved protocols and fed *ad libitum* for 10 weeks, at which point the average weight of the mice was 30.5 ± 2.3 g. Mice were randomly selected for 4 experimental groups: Untreated negative control (1), MRI-treated (6), MRI-control (4), and positive control—exposed to irradiation (3).

2.2. Untreated Negative Control Mouse

One mouse, labeled untreated negative control, was randomly selected to be used as a baseline of γH2AX levels without treatment (*i.e.* radiation, MRI, or extended anesthesia). Blood from this mouse was tested in 6 independent ELISA experiments. The untreated negative control mouse had been previously exposed

to a 10-minute MRI scan unrelated to the experiment and was left to recover for more than 8 days prior to blood extraction and processing. Reports claim if DNA damage were to incur, even during a short MRI scan, this time period would be sufficient for γH2AX levels to return to baseline [9] [11] [18].

2.3. Irradiated Positive Controls

Three mice were randomly selected to be irradiated and serve as a positive control. The blood of one mouse was selected to be treated *ex vivo* by a linear accelerator (LINAC, Elekta Synergy, Canada). Blood was extracted from the mouse via cardiac puncture and immediately transferred to the LINAC where 5 Gy of high-energy X-ray radiation was administered over 5 minutes. The remaining 2 mice were treated with ionizing radiation from a cyclotron during routine production of F-18 with a whole body absorbed dose of either 2 Gy or 10 Gy. Radiation dose for the cyclotron was measured using dosimetry cards (RADTriage Personal Radiation Detector 50 - 10,000 mGy, Nukepills, Edgewater, USA) placed inside the cages. The blood from all irradiated mice was processed 30 minutes after irradiation when the maximum production of γH2AX was expected from literature reports [18].

2.4. Magnetic Resonance Imaging

Ten animals were randomly selected to be placed into one of two in-house developed chambers; One chamber was placed in the MRI bore containing MRI-treated mice (6) while the other was placed outside the 5-Gauss line containing negative control mice (4). Mice were kept under anesthesia with 2% isofluorane (Baxter International Inc., Deerfield, USA) at a controlled temperature of 36˚C for 6 hours. All mice received a 100-μL subcutaneous injection of saline (0.9% Sodium Chloride) to prevent dehydration during experimentation. The chamber containing the mice for MRI-exposure was placed in the center of a 3T MRI bore (Achieva, Philips, The Netherlands) which has a 33 mT/m maximum gradient amplitude and a maximum slew rate of 180 mT/m/s. A single shot echo planar imaging (EPI) sequence was used for scanning the animals in the MRI (TR = 56 ms, TE = 11 ms, FOV = 500 × 500 mm, acquisition matrix = 64 × 63, slice thickness = 320 mm, NEX = 4, dynamic scan time = 0.223 ms). This scan was continuously repeated for a total of 6 hours. Mice from both the MRI-exposure and control groups remained anesthetized during the 6 hours. After the scanning was complete, mice from both groups were randomly selected and sacrificed by cardiac puncture and the blood was used for analysis.

Using the Philips sequence development environment (SDE), the MRI sequence was transferred to a virtual environment where the theoretical slew rate was calculated from system-specific parameters for the sequence gradients strength (mT/m) and corresponding up and down slopes (ms). The theoretical slew rate was calculated by dividing the gradient strength by the slope duration. This resulted in a theoretical slew rate calculation of 192 mT/m/s.

2.5. Blood Sampling and Separation

Mice were placed supine with all 4 legs taped to expose the abdomen and were euthanized under deep anesthesia by cardiac puncture using a 25 g needle with a 3-mL syringe coated with heparin (Fresenius Kabi, #C504710, Heparin Sodium Injection, 10,000 USP units/10 mL) to delay coagulation. The blood from each mouse was transferred from the 3-mL syringe to a 3-mL blood collection tube (BD Vacutainer, REF# 367960, PST Gel and Lithium Heparin).

A mammal lymphocyte separation kit (Lympholyte®-Mammal, CEDARLANE, Cat# CL5110) was used to isolate the peripheral blood mononuclear cells (PBMCs). The separation was performed according to manufacturer's instructions as follows: Approximately 800 µL of blood from each mouse was mixed with equal volume of physiological buffer. Lympholyte was added to a clean 5000 µl tube at twice the volume of the diluted blood sample. Diluted blood was gently added on top of the Lympholyte. The PBMC layer was aspired from the tube after 30 minutes of centrifugation at 400 g. Cells were isolated, washed and lyzed with RIPA buffer (Sigma-Aldrich R0278) containing 1% protease inhibitor cocktail (P8340) and 1% phosphatase inhibitor cocktail (P5726). Lysate was aliquoted and stored at −80˚C.

2.6. Total Protein Concentration of Lysates

The total amount of proteins present in the lysates depends on multiple factors, including individual differences in protein expression, size of the mouse, amount of blood drawn, and efficiency of the cell isolation protocol. In order to equalize the amount of protein in the samples to be analyzed by ELISA, we determined the total amount of protein in each lysate before each ELISA experiment. After thawing the aliquoted lysate, total protein concentration was determined using the Bradford assay (Bradford (1976), Anal. Biochem. 72, 248-254). Coomassie Blue 0.01% w/v solution was prepared using Coomassie Brilliant Blue G-250 in ethanol and phosphoric acid. TBS at pH 7.6 was used as buffer in this assay. A standard curve was constructed in each plate using a serial dilution of bovine serum albumin (BSA) ranging from 0.05 µg/µL to 0.00039 µg/µL. Absorbance was read at 595 nm in a Synergy 4 (Biotek, Inc.) microplate reader. Lysates were diluted by a factor of 4 and plated in triplicate in this assay.

2.7. ELISA Protocol

Lysate concentrations determined by Bradford were used to prepare work solutions of each lysate in dilution buffer (sterile-filtered 1× PBS). The concentration of lysate used in each experiment was kept at the same value for all samples and controls. The presence of γH2AX in the lysates was assayed using sandwich ELISA, as follows: the wells of a clear, high binding, 96-well microplate (Polystyrene Microplates Falcon™, CEDERLANE, CAT# 353072) were coated with 100 µL of capture antibody (Human/Mouse/Rat Histone H2AX monoclonal antibody, host mouse; Novusbio, MAB3406-SP), prepared at 0.004 mg/mL in plating

buffer (sterile-filtered 1× PBS), and incubated overnight at −8˚C. Non-specific binding sites were blocked with the addition of 300 µL of block buffer (TBS pH 7.6 with 1% BSA) per well, followed by 3 hours incubation at room temperature. After blocking, wells were incubated for 3 hours at room temperature with 100 µL of samples, controls, or dilution buffer. Wells were then incubated for 2 hours at room temperature with 100 µL of detection antibody (mouse γH2AX (Ser139) monoclonal antibody conjugated with biotin, host mouse; Upstate, 16-193(CH)) at 0.00125 mg/mL in block buffer. Horseradish peroxidase (HRP) conjugated to streptavidin (Streptavidin-HRP; Biolegend, 405210) at 100 ng/mL was linked to the biotinylated detection antibody (100 µL in each well, incubated for 20 minutes). HRP substrate (1:1 H_2O_2 and tetramethylbenzidine (TMB); R & D Systems, Catalog # DY999) was then added to the wells and incubated for 20 minutes at room temperature. The reaction was stopped by the addition of 50 µL of stop solution (H_2SO_4 at 2N; R&D Systems, Catalog # DY994) to each well. The plate was washed 3 times between treatments with 300 µL wash buffer (TBS pH 7.6 with 0.05% Tween® 20). Absorbance at 450 nm (γH2AX detection), 540 nm (plate correction) and 280 nm were read using a Synergy 4 microplate reader (Biotek, Inc.). Each ELISA experiment was run in duplicate or triplicate.

2.8. Data and Statistical Analyses

Absorbance readings at 450 nm were corrected (Abs) for background absorbance using the average reading from reference wells. Absorbance at 540 nm was read for each well to check for plate imperfections. Absorbance at 280 nm is proportional to the amount of protein and phenolic compounds present in each well and was used to check for well-to-well variations in concentration of both antibodies and antigenic proteins, and other proteins. No correction was necessary for plate imperfection or uneven coating, since the coefficient of variation (CV) between replicates in these readings were all below 10%. For absorbance at 450 nm, a CV of 20% or lower was set as quality control target for technical and biological replicates. Corrected absorbance expressed as percentage of positive control (*ex-vivo* mouse blood irradiated with 5 Gy) was used to combine results from different experiments.

Elisa results are expressed as mean ± SEM, unless otherwise noted. Repeated measures one-way analysis of variance (one-way ANOVA) with Tukey's Multiple Comparison post-test was used for statistical analysis (GraphPad Prism version 5.00 for Windows, GraphPad Software, San Diego California USA, https://www.graphpad.com/). Mean differences were considered statistically significant if $p < 0.05$. GraphPad Prism was used to generate statistical figures and plots.

3. Results and Discussion

3.1. Total Protein Concentration

The concentration of protein in lysates obtained from each mouse was determined using the Bradford method. The average blood collected per mouse was

870 ± 390 μL. Bradford was performed in triplicate before each ELISA and the results were used to prepare ELISA sample solutions at a fixed total protein concentration for each lysate. The average and SEM of all samples was 1 ± 0.35 mg/mL.

3.2. Detection of DNA Breaks

Enzyme-linked Immunosorbent Assay (ELISA) was performed to quantify γH2AX in each sample. γH2AX is a biomarker of DNA double strand breaks and there are published ELISA protocols for its detection. The protocol used in this work was adapted from Ji and co-authors [20]. Their assay detects both Ser 139-phosphorylated and non-phosphorylated H2AX within the same sample. Their approach accounts for individual variations in H2AX expression. Our assay did not account specifically for differences in expression of non-phosphorylated H2AX. However, it did take into account differences in the total amount of protein in each lysate. ELISA is one of the most sensitive types of immunoassays, with a typical detection range of 0.1 ng to 0.01 ng. Although we did not transform our readings in a specific amount of γH2AX, we expect the relative difference between samples and controls to be within typical ELISA detection ranges.

3.2.1. Irradiated Positive Controls

Radiation treated blood (5 Gy) or mice (2 Gy and 10 Gy) were used as positive control samples and to test radiation dose-dependency of the γH2AX ELISA assay. Results shown in **Figure 1** were obtained from multiple ELISA experiments

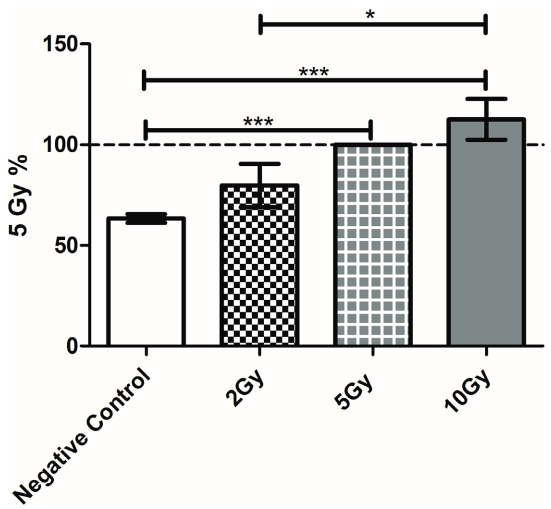

Figure 1. Quantification of γH2AX in positive controls. Bars represent the amount of γH2AX as a percentage of the 5 Gy sample average. Untreated negative control sample (1 mouse, average of 6 independent ELISA experiments, each carried in triplicate) compared to 1 mouse treated with 2 Gy (average of 2 independent ELISA experiments carried in triplicate), 5 Gy (average of 8 independent ELISA experiments, each in triplicate), and 1 mouse treated with 10 Gy (average of 5 independent ELISA experiments each in triplicate). The horizontal bars indicate a statistically significant difference between the means of the two groups connected by the bar, as determined by one-way ANOVA. Three asterisks indicate p values < 0.001 (extremely significant), whereas 1 asterisk indicates p values 0.01 to 0.05 (significant). A radiation dose-dependent increase in γH2AX is observed.

each carried in triplicate, and are expressed as percentage of the 5 Gy readings of each plate. A linear dependency on radiation exposure was observed ($r^2 = 0.93$). One-way analysis of variance (1-way ANOVA) followed by Tukey's comparison of all pairs of columns was performed to compare the treatments shown in **Figure 1**. The differences between 5 Gy and 10 Gy radiation-treated samples and untreated negative control were statistically significant ($p < 0.001$). The difference between 2 Gy and 10 Gy was also statistically significant ($0.01 < p < 0.05$). The two-tailed unpaired t-test p-value for 2 Gy against the negative untreated control was 0.06, slightly above the statistical significance cutoff of 0.05. These results demonstrate that the ELISA assay was able to discriminate between normal and elevated levels of γH2AX induced by radiation of 5 Gy and above when compared to untreated negative control. The relatively small expression increases of γH2AX between the 5 Gy and 10 Gy controls suggest a possible saturation of γH2AX expression. This effect has been well documented by various γH2AX detection methods but shows little consensus on when the relationship between γH2AX expression and absorbed dose is no longer linearly related and becomes saturated [25] [26] [27] [28] [29]. Additionally, it is possible the 10 Gy control received more than 10 Gy absorbed dose due to the dose reporting limitations of the dosimetry card that was maximally exposed.

3.2.2. Presence of γH2AX in Untreated versus MRI-Treated Samples

Lysates obtained from MRI-control and MRI-treated mice were tested at 4 different concentrations, with the corrected absorbance showing a clear concentration trend, confirmed by a 2-way (Treatment, Lysate Concentration) ANOVA (data not shown). Corrected average absorbance from each of 4 independent ELISA experiments was expressed as percentage of the 5 Gy irradiated blood sample and pooled by mouse group. Each independent ELISA experiment was conducted in duplicate (experiment 3) or triplicate (experiments 1, 2 and 4). **Figure 2** shows the average levels of γH2AX detected in each mouse. In **Figure 2**, both MRI-treated and MRI-control groups are distinct from 5 and 10 Gy-treated mice, but roughly equivalent to each other.

To quantitatively compare the groups, mean and SEM of the biological replicates in each category were calculated and are shown in **Figure 3**. Repeated measures 1-way ANOVA indicates that the differences between the means of 10 Gy irradiated positive control and MRI-control samples are statistically significant. The difference between the means of the MRI-treated and MRI-control samples was not statistically significant but shows a small difference resulting from lower than average levels of γH2AX in one of the mice. Moreover, the MRI-treated mean is statistically lower than irradiated controls, indicating extensive exposure to high slew rates in MRI did not cause DSBs comparable to the radiation-treated controls.

Typical MRI scanning times per patient are around 45 - 60 minutes [30]. The slew rate during clinical use varies with the type of scan performed but ranges from 5 mT/m/s to a maximum of 180 mT/m/s. Thermometry acquisitions and

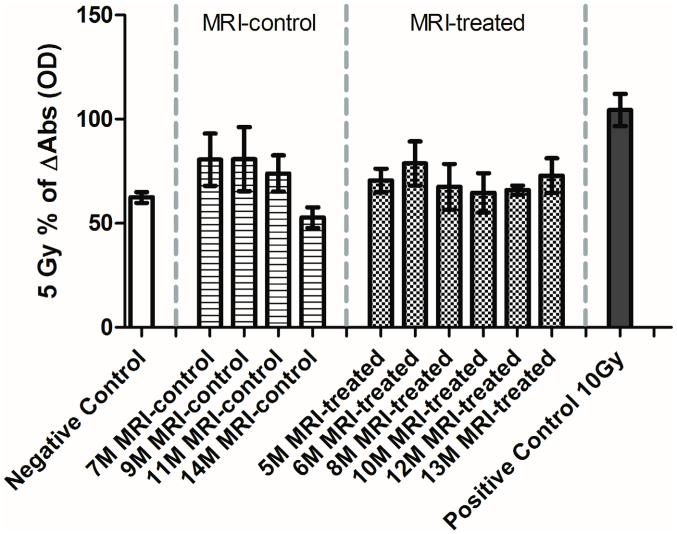

Figure 2. Mean γH2AX Exposure per Individual Biological Replicate. Mean and SEM of 4 ELISA experiments per individual biological replicate for each treatment category, expressed as percentage of the irradiated 5 Gy positive control. Categories are: untreated negative control (1 mouse), MRI-control (4 mice), MRI-treated (6 mice), positive control 10 Gy (1 mouse).

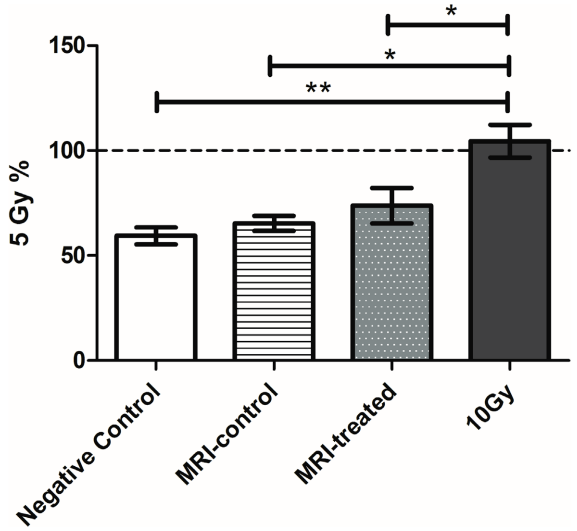

Figure 3. Presence of γH2AX in biological replicates of untreated and MRI-treated mice. Bars represent mean and SEM values of untreated negative control (1 mouse), MRI-control (4 mice), MRI-treated (6 mice), and 10 Gy irradiated (1 mouse) samples. The amount of γH2AX in each sample was averaged over 4 independent ELISA experiments, each conducted in duplicate or triplicate. The horizontal bars indicate a statistically significant difference between the means of the two groups, as determined by one-way ANOVA. Two asterisks indicate p values 0.001 to 0.01, whereas 1 asterisk indicates p values 0.01 to 0.05. There is no statistically significant difference between MRI-treated and MRI-control animals.

sequences using EPI are examples of sequences utilize higher slew rates. The slew rate used during our work was much higher with a longer exposure than that normally used in clinical MRI. This caused the MRI exposure from our

work to be significantly higher than the ones used in studies that reported DNA damage due to MRI. A limitation of our study is the detection sensitivity of γH2AX suggested by **Figure 1** where there is no statistical difference between the negative control and 2 Gy positive control. An earlier study developed the γH2AX ELISA method [20] which suggested high detection sensitivity of γH2AX expression as a function of absorbed dose, but analyzed γH2AX expression in tissue samples instead of blood. It is possible variability in blood processing and collection of PBMCs reduced our sensitivity to γH2AX expression. Regardless, if DSBs were to occur as a result of MRI gradient exposure, as previously reported [3], this acute MRI exposure should have been sufficient to produce significant DNA damage. Since no significant DNA damage between the MRI-treated and MRI-control groups was detected in our experiments as a result of acute MRI exposure, it is reasonable to conclude that exposure to standard clinical MRI is unlikely to cause DSBs.

4. Conclusion

Conflicting reports in literature justify the need to determine if exposure to MRI can cause DSBs. An enzyme-linked immunosorbent assay (ELISA) to detect γH2AX was used to determine the amount of γH2AX produced as a result of treatment, which correlates with the extent of double stranded breaks (DSBs) in DNA. We compared the γH2AX levels in mice exposed to a 6-hour continuous MRI scan with high slew rate to mice not exposed to MRI and to a positive control obtained with ionizing radiation. The MRI exposure used was in excess of what typically is used during routine clinical imaging. We found that the amount of γH2AX in samples undergoing long MRI scans was statistically indistinguishable from samples that were maintained in the same general environment but were not scanned. Our results suggest that exposure to MRI is unlikely to be a major source of DNA breakage. However, our experimental design did not account for potential DNA damage caused by factors associated to pre-experiment preparation (e.g., stress, anesthesia, noise). We speculate that the DSBs observed in other studies are likely associated to other sources such as contrast agents, stress, anesthesia, or noise, rather than the magnetic field and radiofrequency pulses used in MRI. Future studies would also include treatment groups to further isolate the effect of MRI contrast agents on DSBs. This work demonstrated a proof of concept where future work would utilize a stronger statistical power.

Conflicts of Interest

The authors declare no conflicts of interest regarding the publication of this paper.

References

[1] Khanna, K.K. and Jackson, S.P. (2001) *Nature Genetics*, **27**, 247-254. https://doi.org/10.1038/85798

[2] Foster, K.R., Moulder, J.E. and Budinger, T.F. (2017) *Radiation Research*, **187**, 1-6.

https://doi.org/10.1667/RR14529.1

[3] Fiechter, M., Stehli, J., Fuchs, T.A., Dougoud, S., Gaemperli, O. and Kaufmann, P.A. (2013) *European Heart Journal*, **34**, 2340-2345. https://doi.org/10.1093/eurheartj/eht184

[4] Fraum, T.J., Ludwig, D.R., Bashir, M.R. and Fowler, K.J. (2017) *Journal of Magnetic Resonance Imaging*, **46**, 338-353. https://doi.org/10.1002/jmri.25625

[5] Rogosnitzky, M. and Branch, S. (2016) *BioMetals*, **29**, 365-376. https://doi.org/10.1007/s10534-016-9931-7

[6] Simi, S., Ballardin, M., Casella, M., De Marchi, D., Hartwig, V., Giovannetti, G., *et al.* (2008) *Mutation Research/Fundamental and Molecular Mechanisms of Mutagenesis*, **645**, 39-43. https://doi.org/10.1016/j.mrfmmm.2008.08.011

[7] Yildiz, S., Cece, H., Kaya, I., Celik, H., Taskin, A., Aksoy, N., *et al.* (2011) *Clinical Biochemistry*, **44**, 975-979. https://doi.org/10.1016/j.clinbiochem.2011.05.005

[8] Lee, J.W., Kim, M.S., Kim, Y.J., Choi, Y.J., Lee, Y. and Chung, H.W. (2011) *Bioelectromagnetics*, **32**, 535-542. https://doi.org/10.1002/bem.20664

[9] Fatahi, M., Reddig, A., Vijayalaxmi, F.B., Hartig, R., Prihoda, T.J., *et al.* (2016) *NeuroImage*, **133**, 288-293. https://doi.org/10.1016/j.neuroimage.2016.03.023

[10] Reddig, A., Fatahi, M., Roggenbuck, D., Ricke, J., Reinhold, D., Speck, O., *et al.* (2016) *Radiology*, **2016**, Article ID: 160794. https://doi.org/10.1148/radiol.2016160794

[11] Reddig, A., Fatahi, M., Friebe, B., Guttek, K., Hartig, R., Godenschweger, F., *et al.* (2015) *PLOS ONE*, **10**, e0132702. https://doi.org/10.1371/journal.pone.0132702

[12] Lancellotti, P., Nchimi, A., Delierneux, C., Hego, A., Gosset, C., Gothot, A., *et al.* (2015) *Circulation*, *Cardiovascular Imaging*, **8**, e003697. https://doi.org/10.1161/CIRCIMAGING.115.003697

[13] Schreiber, W.G., Teichmann, E.M., Schiffer, I., Hast, J., Akbari, W., Georgi, H., *et al.* (2001) *Journal of Magnetic Resonance Imaging*, **14**, 779-788. https://doi.org/10.1002/jmri.10010

[14] Ivashkevich, A., Redon, C.E., Nakamura, A.J., Martin, R.F. and Martin, O.A. (2012) *Cancer Letters*, **327**, 123-133. https://doi.org/10.1016/j.canlet.2011.12.025

[15] Redon, C.E., Nakamura, A.J., Sordet, O., Dickey, J.S., Gouliaeva, K., Tabb, B., *et al.* (2011) γ-H2AX Detection in Peripheral Blood Lymphocytes, Splenocytes, Bone Marrow, Xenografts, and Skin. In: Didenko, V.V., Ed., *DNA Damage Detection in Situ*, *ex Vivo*, *and in Vivo*, Humana Press, Totowa, 249-270. http://link.springer.com/10.1007/978-1-60327-409-8_18 https://doi.org/10.1007/978-1-60327-409-8_18

[16] Burma, S. (2001) *Journal of Biological Chemistry*, **276**, 42462-42467. https://doi.org/10.1074/jbc.C100466200

[17] Rogakou, E.P., Pilch, D.R., Orr, A.H., Ivanova, V.S. and Bonner, W.M. (1998) *Journal of Biological Chemistry*, **273**, 5858-5868. https://doi.org/10.1074/jbc.273.10.5858

[18] Rube, C.E., Grudzenski, S., Kuhne, M., Dong, X., Rief, N., Lobrich, M., *et al.* (2008) *Clinical Cancer Research*, **14**, 6546-6555. https://doi.org/10.1158/1078-0432.CCR-07-5147

[19] Bonner, W.M., Redon, C.E., Dickey, J.S., Nakamura, A.J., Sedelnikova, O.A., Solier, S., *et al.* (2008) *Nature Reviews Cancer*, **8**, 957-967. https://doi.org/10.1038/nrc2523

[20] Ji, J., Zhang, Y., Redon, C.E., Reinhold, W.C., Chen, A.P., Fogli, L.K., *et al.* (2017) *PLOS ONE*, **12**, e0171582. https://doi.org/10.1371/journal.pone.0171582

[21] Bourton, E.C., Plowman, P.N., Zahir, S.A., Senguloglu, G.U., Serrai, H., Bottley, G.,

et al. (2012) *Cytometry Part A*, **81**, 130-137. https://doi.org/10.1002/cyto.a.21171

[22] Matsuzaki, K., Harada, A., Takeiri, A., Tanaka, K. and Mishima, M. (2010) *Mutation Research/Genetic Toxicology and Environmental Mutagenesis*, **1**, 71-79. https://doi.org/10.1016/j.mrgentox.2010.05.009

[23] Redon, C.E., Nakamura, A.J., Zhang, Y.-W., Ji, J., Bonner, W.M., Kinders, R.J., *et al.* (2010) *Clinical Cancer Research*, **16**, 4532-4542. https://doi.org/10.1158/1078-0432.CCR-10-0523

[24] Johnston, M.L., Young, E.F. and Shepard, K.L. (2015) *Radiation and Environmental Biophysics*, **54**, 365-372. https://doi.org/10.1007/s00411-015-0595-4

[25] Rothkamm, K. and Horn, S. (2009) *Annali dell'Istituto Superiore di Sanità*, **45**, 265-271.

[26] Rothkamm, K. and Löbrich, M. (2003) *Proceedings of the National Academy of Sciences*, **100**, 5057-5062. https://doi.org/10.1073/pnas.0830918100

[27] Macphail, S.H., BanÁth, J.P., Yu, T.Y., Chu, E.H.M., Lambur, H. and Olive, P.L. (2003) *International Journal of Radiation Biology*, **79**, 351-359. https://doi.org/10.1080/0955300032000093128

[28] Andrievski, A. and Wilkins, R.C. (2009) *International Journal of Radiation Biology*, **85**, 369-376. https://doi.org/10.1080/09553000902781147

[29] Markova, E., Torudd, J. and Belyaev, I. (2011) *International Journal of Radiation Biology*, **87**, 736-745. https://doi.org/10.3109/09553002.2011.577504

[30] UCSF Radiology (2019) Prepare for Magnetic Resonance Imaging (MRI) https://radiology.ucsf.edu/patient-care/prepare/mri